ACS OMEGA

Open Access

http://pubs.acs.org/journal/acsodf

Article

Catalytic Decomposition of an Organic Electrolyte to Methane by a Cu Complex-Derived In Situ CO_2 Reduction Catalyst

Kyuman Kim, Pawel Wagner, Klaudia Wagner, and Attila J. Mozer*

Cite This: *ACS Omega* 2023, 8, 41792−41801

Read Online

ACCESS | Metrics & More | Article Recommendations | Supporting Information

ABSTRACT: Metal complexes are often transformed to metal complex-derived catalysts during electrochemical CO_2 reduction, enhancing the catalytic performance of CO_2 reduction or changing product selectivity. To date, it has not been investigated whether metal-complex derived catalysts also enhance the decomposition of the solvent/electrolyte components as compared to an uncoated electrode. Here, we tested the electrochemical stability of five organic solvent-based electrolytes with and without a Cu complex-derived catalyst on carbon paper in an inert atmosphere. The amount of methane and hydrogen produced was monitored using gas chromatography. Importantly, the onset potential for methane production was reduced by 300 mV in the presence of a Cu complex-derived catalyst leading to a significant amount of methane (417.7 ppm) produced at −2.17 V vs Fc/Fc^+ in acetonitrile. This suggests that the Cu complex-derived catalyst accelerated not only CO_2 reduction but also the reduction of the electrolyte components. This means that Faradaic efficiency (FE) measurements under CO_2 in acetonitrile may significantly overestimate the amount of CH_4. Only 28.8 ppm of methane was produced in dimethylformamide under an inert atmosphere, much lower than that produced under CO_2 (506 ppm under CO_2) at the same potential, suggesting that dimethylformamide is a more suitable solvent. Measurements in propylene carbonate produced mostly hydrogen gas while in dimethyl sulfoxide and 3-methoxypropionitrile neither methane nor hydrogen was detected. A strong linear correlation between the measured current and the amount of methane produced with and without the Cu complex-derived catalyst confirmed that the origin of methane production is solvent/electrolyte decomposition and not the decomposition of the catalyst itself. The study highlights that in a nonaqueous system, highly active catalyst in situ deposited during electrochemical testing can significantly influence background measurements as compared to uncoated electrodes, therefore the choice of solvent is paramount for reliable testing.

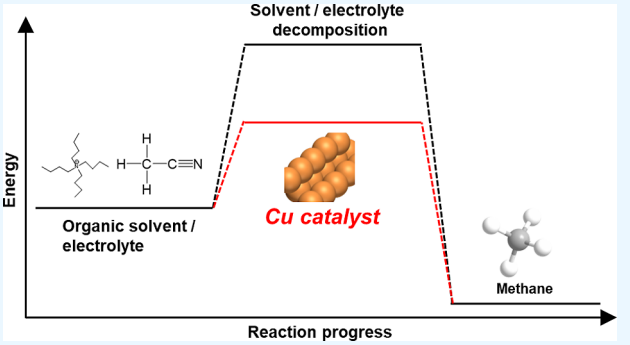

INTRODUCTION

The reliable characterization of the electrochemical CO_2 reduction performance of metal complex catalysts almost always includes measurements of product selectivity and Faradaic efficiency (FE).[1,2] FE of the various products, defined as the percentage of electrons consumed to form the specific product (output) to the total charge flowing in the electrochemical system (input), $\text{FE}\,(\%) = \frac{Q_{\text{output}}}{Q_{\text{input}}} \times 100$, is one of the most important characteristics that help uncovering possible mechanisms and production pathways. To determine FE of gas products, a gas chromatograph is often directly connected to the electrochemical cell at the gas outlet to measure the identity and quantity of gas products every 20 min to 1 h intervals during the electrolysis, depending on the specific gas chromatograph used. Gas chromatography (GC) performs quantitative and qualitative analysis of gas products during electrolysis using calibration values made by known amount of gases.[3] A problem arises if a specific reduction product, i.e. methane, is produced by reactions other than CO_2 reduction, such as the decomposition of solvent and/or the supporting electrolyte, working electrode, catalyst, or other components used to prepare the electrochemical cell. For reliable characterization of new catalysts, it is necessary to separate the background gas production from the gas produced from CO_2.

To check if other reactions contribute to the generation of the monitored products, electrolysis in an inert atmosphere (N_2 or argon) using a metal complex catalyst is routinely measured.[4] Typically, the same working electrode such as a carbon electrode is measured in inert gas and compared to the

Received: August 28, 2023
Revised: September 27, 2023
Accepted: September 28, 2023
Published: October 27, 2023

measurements performed under CO_2 with the metal complex present in the electrolyte. The difference in gas production, in principle, can be attributed to products generated by CO_2 reduction. However, metal complexes often transform to metal complex-derived catalysts during electrolysis, especially Cu complexes with tetragonal geometries.[3] These in situ formed catalysts often have different catalytic active sites leading to different mechanisms as compared to the metal complex originally introduced.[3] For example, demetalation of Cu complexes may lead to a ligand-based polymeric organic phase and a metallic Cu phase.[5] The newly formed Cu complex-derived catalyst often produces methane (CH_4) with high selectivity, while the original Cu complex in solution typically produces two electron products CO and HCOOH. The most important step in the CO_2 reduction to CH_4 is the hydrogenation of adsorbed CO (*CO) to adsorbed formyl CHO (*CHO), which should take place prior to releasing the CO from the active site.[6] The restructured Cu complex-derived catalyst may have a lower Cu−Cu coordination number than the original Cu complex, lowering the reaction energy of the hydrogenation step of *CO.[7] The organic phase composed of the ligands, adjacent to the Cu sites, may bind and thus enhance the hydrogenation of *CO.[8]

In the last five years, in situ and in operando X-ray absorption spectroscopic techniques revealed such restructuring of Cu complexes to Cu complex-derived catalysts in aqueous solution.[7,9,10] Nevertheless, such in situ measurements of Cu complex-derived catalysts are rare in organic solvents. Furthermore, determination of product selectivity and FE for the electrochemical reduction of CO_2 in organic solvents is problematic due to background CH_4 production by solvent/electrolyte decomposition.[11] While solvent/electrolyte decomposition in an aqueous system leads to hydrogen gas, the decomposition of organic electrolytes may lead to carbonous gases that can overlap with products of CO_2 reduction.

Organic solvents have been traditionally employed for electrochemical CO_2 reduction for over 4 decades due to high solubility of several important class of ligands, high solubility of CO_2, and easily tunable (by choice of wide range of solvents) dielectric constant.[12,13] Organic solvents chosen for CO_2 reduction experiments should be electrochemically stable at high cathodic potentials where CO_2 reduction reactions typically occur so that interference with the CO_2 reduction process can be avoided. Acetonitrile (ACN), *N*,*N*-dimethylformamide (DMF), dimethyl sulfoxide (DMSO), and propylene carbonate (PC) are the most commonly used solvents for catalysis using metal complex catalysts due to their wide cathodic electrochemical window (over −3.0 V vs Fc/Fc^+) and good solubility of the complexes.[14] However, the decomposition of organic solvents/electrolyte components to byproducts including methane and ethane has been reported.[11,15−19] Ue et al. defined the upper negative potential stability limit of ACN with a tetraethylammonium tetrafluoroborate supporting electrolyte (0.65 M) as the potential where the current density reached 1 mA cm^{-2} at a scan rate of 5 mV s^{-1}.[20] The measured upper limit was −3.3 V vs Fc/Fc^+ when the working electrode was the glassy carbon electrode.[20] However, Hoshi et al. reported the formation of methane on a platinum working electrode attributed to solvent decomposition in TBAP/ACN with 0.1 M chlorobenzene and 0.42 M H_2O at a lower potential (at −3.02 V vs Fc/Fc^+) than that determined by Ue et al.[18,20] Methane was not generated in the TBAP/THF at the same potential.[18] ACN decomposing to form the methyl radical ($^{\bullet}CH_3$) and cyanide ion (CN^-) followed by the methyl radical reacting with H^+ from water molecules was the proposed pathway to generate methane. Methane formation by solvent/electrolyte decomposition was also reported in the presence of metal complex catalysts. Simpson and Durand found small amount of methane produced by the decomposition of electrolyte tetrabutylammonium tetrafluoroborate ($TBABF_4$/DMSO) using metal (Co, Ni and Cu) phenanthroline complexes.[11]

Recently, we developed a Cu complex-derived catalyst, consisting of a metallic Cu phase and possibly a polymeric organic phase, deposited in situ during the electrolysis of a dimethyl-substituted phenanthroline (2,9-dimethyl-1,10-phenanthroline−neocuproine, dmp) Cu^{2+} complex dissolved in 0.1 M tetrabutylammonium perchlorate (TBAP)/DMF solution with 0.1 M water.[21] The Cu complex-derived catalyst performed highly selective (up to 80% FE) methane production. The amount of CH_4 produced under a CO_2 atmosphere using an uncoated carbon paper electrode was negligible at the same applied potential. However, the question arises whether the in situ deposited Cu complex-derived catalyst also catalyzes solvent/electrolyte decomposition, i.e., what is the amount of CH_4 generated in an inert atmosphere when the carbon electrodes are coated with the catalyst? To answer this question and, more generally, to investigate the stability of various commonly used solvent/electrolyte systems with our in situ formed catalyst, we have prepared Cu complex-derived catalyst in the TBAP/DMF electrolyte in nominally identical conditions and then compared the catalytic activity toward solvent/electrolyte decomposition of five different organic solvents with a 0.1 M TBAP supporting electrolyte. DMF, ACN, DMSO, 3-methoxypropionitrile (MPN), and PC are chosen due to their general electrochemical stability and common use in similar experiments.[14,22] First, cyclic voltammetry (CV) was performed using the Cu complex-derived catalysts in the five different solvents in an argon atmosphere, and the results were compared to the CVs recorded only with the uncoated carbon paper electrode. Then, chronoamperometry (CA) was carried out with and without the Cu complex-derived catalyst at three different potentials. The gas products generated during CA were measured by using GC. The structural transformation of Cu-based catalysts has been reported during CO_2 reduction experiments leading to the loss of CO_2 reduction performance.[23,24] In contrast, some Cu-based catalysts showed increased selectivity toward hydrocarbons following catalyst restructuring.[25−27] Such catalyst restructuring may also occur during "background" measurements, i.e., during CA under an inert atmosphere. We have compared the electrochemical characteristics (CVs) and the morphology of the in situ-deposited catalyst using X-ray diffraction (XRD) and scanning electron microscopy (SEM) before and after the chronoamperometric testing.

EXPERIMENTAL SECTION

Materials. DMF (RCI Labscan, 99.8%), ACN (Sigma-Aldrich, 99.8%), MPN (Sigma-Aldrich, 99%), DMSO (chemsupply, 99%), PC (Sigma-Aldrich, 99%), and TBAP (Sigma-Aldrich, 98%) were commercially obtained. The dimethylphenanthroline complex $[Cu(II)(dmp)_2](TFSI)(Cl)$ was prepared by following a previous report.[28]

In Situ Electrodeposition of the Cu Complex-Derived Catalyst on Carbon Paper Electrodes. The Cu complex-derived catalyst was fabricated by in situ electrodeposition in a

https://doi.org/10.1021/acsomega.3c06440
ACS Omega 2023, 8, 41792−41801

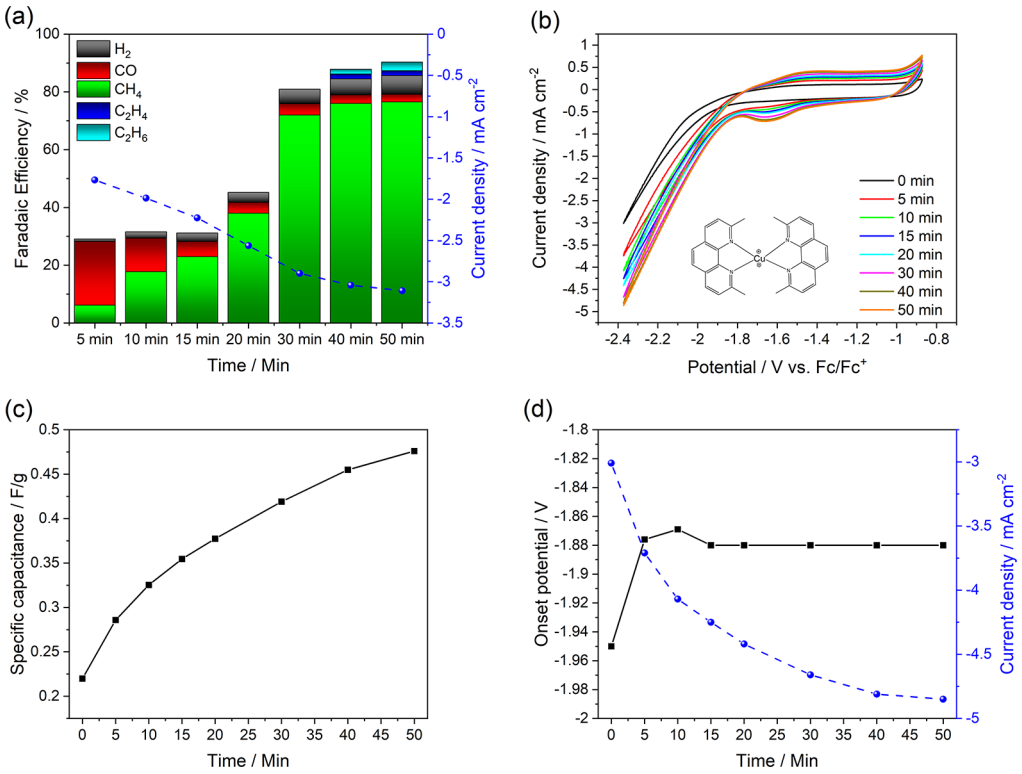

Figure 1. (a) FE of gas products (bar graph) and current density (line graph) during CA, (b) CV curves during electrodeposition in DMF with 0.1 M TBAP in CO_2, (c) specific capacitance during CA, and (d) onset potentials and current density at −2.37 V during CA.

three-electrode, two-compartment electrochemical cell (Pine Instruments, USA) by a potentiostat (650D, CH Instrument). A platinum mesh was employed as the counter electrode in a compartment. A carbon paper (36AA, FuelCellStore Sigracet, USA) was used as the working electrode in another compartment separated by a glass frit. To prepare the carbon paper electrode, a piece of carbon paper was connected to the instrument cable by copper tape. To limit the exposure of the copper tape to the electrolyte, the copper tape was then fully covered by silicone glue (see Figure S4). The carbon paper electrode was prepared at least 24 h before the electrochemical measurement to allow for the complete curing of the silicon glue. $Ag/AgNO_3$ was used as the reference electrode, placed in the same compartment with the working electrode. The surface area of the carbon paper was 1 × 1.5 cm^2. The electrolyte for electrodeposition of the catalyst contained 1 mM dmp-Cu complexes dissolved in DMF, 0.1 M TBAP, and 0.1 M water. Before measurement, the cathodic chamber was purged with CO_2 for 30 min, and the applied potential was −2.17 V vs Fc/Fc^+ for 80 min. CO_2 gas was continuously bubbled at 15 mL/min, and the solution was stirred at 300 rpm during electrodeposition.

Electrochemical Measurements of Solvent/Electrolyte Decomposition Using the In Situ Deposited Catalyst. Electrochemical measurements were performed by using the same three-electrode setup. The electrodeposited Cu complex-derived catalyst on carbon paper was used as the working electrode, and the same reference and counter electrodes were used as above. Five different solvents (DMF, ACN, DMSO, MPN, and PC) with 0.1 M TBAP and 0.1 M water were employed as electrolytes. All potentials in this study were adjusted to the potential versus Fc/Fc^+ added as an internal standard. Before the measurement, the cathodic chamber was purged with argon for 30 min. The electrolyte solutions were continuously stirred at 300 rpm, while argon gas was bubbled at a 15 mL/min flow rate. The gaseous products were measured through the gas outlet of the electrochemical cell with a gas chromatograph (GC2030, Shimadzu, Japan) equipped with thermal conductivity and flame ionization detectors. The amount of gas products was calculated by using in-house calibration curves of known volumes of H_2, CO, CH_4, C_2H_4, and C_2H_6 gases.

Correlation Analysis. To understand the origin of methane production under an inert atmosphere, Pearson correlation coefficients (R) were calculated by using OriginPro 2021 between the measured current densities and the amount of methane produced. R means the strength of linear correlations between two parameters with values between −1 and +1. A value closer to +1 indicates a strong positive linear correlation, while a value closest to −1 means a strong negative linear correlation.

Liquid Products. We note that liquid products could not be detected with our experimental setup.

RESULTS AND DISCUSSION

Figure 1 shows the current measured during CA of 1 mM dmp-Cu (II) complexes dissolved in 0.1 M TBAP in a DMF solution with 0.1 M deionized (DI) water added. The cathode compartment of the electrochemical cell was purged with CO_2 at a flow rate of 15 mL per minute. As Figure 1a also shows, within the first five min, a small amount of carbon monoxide (CO) was produced. Assuming that the CO and CH_4 were generated from the electrochemical reduction of CO_2, the FE for CO was calculated as 22%. The FE for CO production decreased from 22 to 2.6% as time progressed, while methane production gradually increased from 6 to 38% (20 min) and

https://doi.org/10.1021/acsomega.3c06440
ACS Omega 2023, 8, 41792−41801

72% (30 min) with a concurrent increase in the current density. Eventually, FE for methane reached 76.5% after 50 min. C_2H_4 and C_2H_6 were also detected with a FE of 1.64 and 3.03%, respectively. Du et al. recently reported that phenanthroline-based Cu complexes transformed to Cu complex-derived catalysts during CA in an aqueous solution. The Cu complex-derived catalyst performed selective ethylene production.[29] As we have shown previously, the catalyst layer consisting of metallic copper and possibly an organic phase was in situ deposited during the chronoamperometric testing under a CO_2 atmosphere.[21] The in situ formation of the catalyst layer was followed by CV measured repeatedly during chronoamperometric testing every 5−10 min (Figure 1b). The CV curves show new redox peaks appearing at −1.4 and −1.65 V attributed to the in situ deposition of a Cu complex-derived catalyst starting after 5 min and with gradually increasing peaks up to 50 min. In addition, the capacitance of the samples (current measured between −1.2 and −1.0 V) continuously increased (Figure 1c). The specific capacitance was calculated using eq 1 as[30]

$$C_m = \frac{\int i dv}{2m \times \Delta V \times v} \quad (1)$$

where $\int i dv$ is the integrated area of the CV curves; m is the mass of the carbon paper electrode (10 mg); ΔV is the scanned potential window (0.2 V); and v is the scan rate (100 mV/s). Integrated area of the CV curves was between −1.2 to −1.0 V vs Fc/Fc^+.

The onset potential, determined as the intersection of the fast-rising current component and the capacitive current, was shifted to positive in the first 15 min and then it was almost constant until the end of chronoamperometric testing. The current density at −2.37 V continuously increased (Figure 1d). The source of the current in CV curves can be divided into three main components. The increasing capacitive current at lower potentials is related to a growth of a conducting layer due to the in situ deposition of a catalyst with an increasing accessible surface area. The redox peaks are assigned to reduction/oxidation of this electroactive catalyst layer. Third, the onset of current > 1.8 V could be attributed to current due to CO_2 reduction/and or electrolyte degradation.

As the FE measurements indicate, close to 80% of the current at −2.02 V vs Fc/Fc^+ was associated with the production of methane toward the end of testing when the catalyst layer was fully developed. However, in these in situ measurements, it is not possible to separate CO/CH_4 generated by electrochemical CO_2 reduction from the decomposition of the Cu dmp complex, the solvent/electrolyte, or any other components of the electrochemical cell. To separate the various possible sources of methane production, we prepared five nominally identical samples of the Cu complex-derived catalyst on carbon paper, rinsed in DMF and dried to remove any physically absorbed Cu complexes (see Figure S2). Then, the electrodes were tested in fresh electrolyte solutions in five different solvents without the Cu complexes added to the electrolytes. The chronoamperograms showed similar current densities and a similar total charge of 7.9 ± 0.73C for these five samples. The CV curves of the five samples after Cu complex-derived catalyst deposition measured in DMF as the electrolyte were nearly identical, suggesting the similar electronic nature and surface area of the catalyst (Figure S1b).

Next, the five identically prepared electrodes were measured by CV under an inert argon atmosphere in five different solvent-based electrolytes and compared to uncoated carbon paper electrodes. Figure 2 shows the fifth cycle (see five

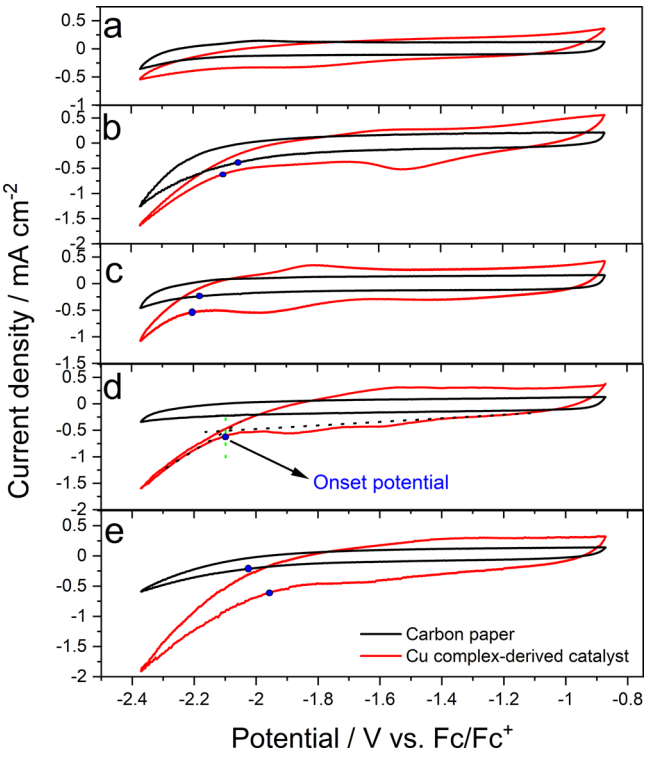

Figure 2. CV curves and onset potentials (blue dot) of Cu complex-derived catalysts and carbon paper in five different organic solvents: (a) DMSO, (b) MPN, (c) DMF, (d) ACN, and (e) PC in argon.

consecutive cycles in Figure S3) of current density versus potential curves in (a) DMSO, (b) MPN, (c) DMF, (d) ACN, and (e) PC also containing 0.1 M TBAP and 0.1 M DI water in argon. Generally, in all five solvents, the currents have increased using the Cu complex-derived catalyst as compared to uncoated carbon paper electrodes but not to the same extent (Table 1). In ACN and PC, the current density using the Cu complex-derived catalyst has increased the most, 4 to 5 times, indicating a more pronounced electrolyte decomposition. Generally, the onset potentials were around −2.1 V vs Fc/Fc^+ for all solvents studied (See Table 1), except in PC it was −1.95 V vs Fc/Fc^+.

Table 1. Onset Potentials and Current Densities at −2.37 V vs Fc/Fc^+ of the Cu Complex-Derived Catalyst and Carbon Paper Electrode in Different Solvents

		onset potential (Fc/Fc^+)		current density at −2.37 V (mA cm^{-2})	
no.	solvent	carbon paper	Cu complex-derived catalyst	carbon paper	Cu complex-derived catalyst
a	DMSO			−0.36	−0.53
b	MPN	−2.05	−2.1	−1.25	−1.63
c	DMF	−2.18	−2.2	−0.44	−1.08
d	ACN		−2.1	−0.33	−1.6
e	PC	−2.02	−1.95	−0.59	−1.90

https://doi.org/10.1021/acsomega.3c06440
ACS Omega 2023, 8, 41792−41801

Carbon paper itself is generally considered catalytically inactive for solvent/electrolyte decomposition and hydrogen evolution.[31] The relatively flat CV curves within the measured potential window using carbon paper electrodes in DMSO, DMF, and ACN suggest only minimal electrochemical reactions. However, clear current onsets were observed using carbon paper electrodes in MPN and PC, indicating electrolyte decomposition, even without a catalyst layer. The increased current using the Cu complex-derived catalyst compared to that of the carbon paper electrode has two possible origins. In DMSO, MPN, DMF, and PC, the onset potentials using the Cu complex-derived catalyst are largely unchanged (Table 1) indicating no catalytic enhancement. The increased current in these cases can be attributed to the larger surface area of the catalyst as compared with the carbon paper electrode (Figure 1c). In ACN, however, the appearance of onset potential using the Cu complex-derived catalyst clearly indicates catalytically enhanced electrolyte decomposition. The origin of increased current in all cases could in principle be assigned to the decomposition of the catalyst layer itself. To identify the possible origin, we performed chronoamperometric testing at various potentials (−2.02, −2.17, and −2.47 V vs Fc/Fc^+) and used a gas chromatograph to detect gaseous products simultaneously.

Figure 3 compares the chronoamperograms of uncoated carbon paper electrodes with that of the Cu complex-derived catalyst in five different solvents in argon. The amount of gas detected at 60 min and the total charge during CA are listed in Table 2.

The total charge during CA measured for carbon paper electrodes (Figure 3) at −2.02 and −2.17 V were generally consistent with the CV curves in Figure 2, showing increasing charge in the order of DMSO, DMF, MPN, and ACN/PC. At −2.47 V (beyond the range of the CV measurement in Figure 2), the total charge in ACN and MPN increased significantly to 7.14 and 11.84C, respectively, while in PC it remained comparatively low and similar to that of in DMF and DMSO.

The amount of total charge collected in CA using the Cu complex-derived catalyst at −2.02 and −2.17 V in DMSO, DMF, MPN, PC, and ACN was a factor of 2 to 3 times higher than measured using carbon paper electrodes. The order of increasing charge followed the same order as that using carbon paper electrodes. However, the total charge in ACN at −2.17 V was over 6 times higher using the Cu complex-derived catalyst as compared to a carbon paper electrode. At −2.47 V, the total charge using the Cu complex-derived catalyst in all solvents was over 5 times higher than that of carbon paper electrodes except in DMSO, in which the charge was the same at both voltages.

In DMF and ACN, methane (CH_4) was the main gas product detected by the gas chromatograph. In PC, hydrogen (H_2) was detected with close to 100% FE. Note that our capability would also allow the detection of CO, C_2H_4, and C_2H_6. We focus our attention to methane detection under an inert argon atmosphere as it can interfere with the FE measurements in CO_2 reduction experiments. Table 2 lists the amounts of methane produced at three different potentials. Surprisingly, a significant amount of methane (16.3 to 355 ppm) was detected in chronoamperometric measurements using a carbon paper electrode in ACN, although the CV curves were relatively flat without an obvious current onset when scanned up to −2.37 V (Figure 2). The amount of methane detected in DMF was negligible (max 1.92 ppm at

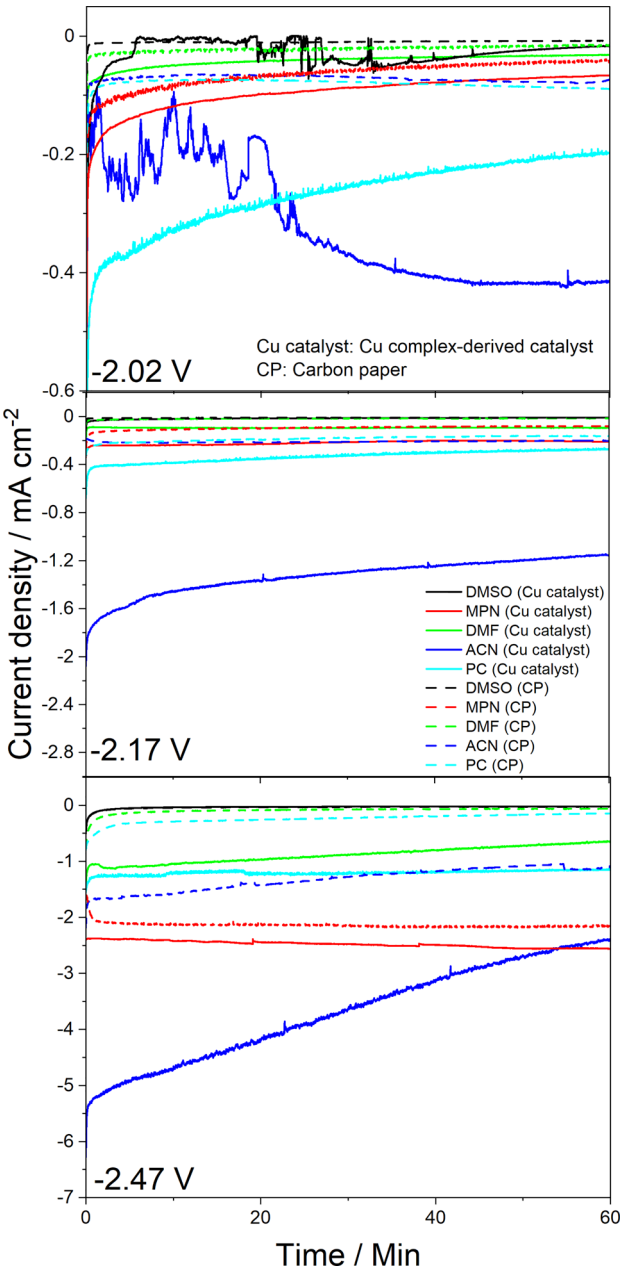

Figure 3. Chronoamperograms of the Cu complex-derived catalyst and carbon paper electrode at three different potentials (−2.02, −2.17, and −2.47 V) in argon.

−2.47 V). Even though the carbon paper electrode in MPN exhibited a significant current onset (total charge, 11.84C) at −2.47 V, no gaseous products were detected.

Using the Cu complex-derived catalyst, similarly to carbon paper, methane gas was detected in DMF and ACN while in other solvents no or very low level of methane was detected (less than 1 ppm). Small amount of H_2 was also produced at −2.47 V in ACN, but the FE was lower than 5%.

The amount of gas products generated using the Cu complex-derived catalyst has increased as compared to using carbon paper electrodes in DMF (from 0.11 to 5.43 ppm, from 0.09 to 28.85 ppm and 1.92 to 296.4 ppm at −2.02, −2.17, and −2.47 V, respectively). However, the amount of charge increased less prominently, from 0.1 to 0.23C, from 0.1 to 0.52C, and from 0.5 to 5.83C at the same potentials,

https://doi.org/10.1021/acsomega.3c06440
ACS Omega 2023, 8, 41792−41801

Table 2. Total Charge Collected during CA and the Amount of Methane Detected at 60 min of CA in Argon on the Cu Complex-Derived Catalyst and Carbon Paper Electrode at Three Different Potentials (−2.02, −2.17, and −2.47 V vs Fc/Fc^+)

solvent	electrode	CH_4 (ppm) at −2.02 V	total charge collected at −2.02 V(C)	CH_4 (ppm) at −2.17 V	total charge collected at −2.17 V(C)	CH_4 (ppm) at −2.47 V	total charge collected at −2.47 V(C)
DMSO	carbon paper	0.15	0.05		0.06	0.45	0.21
MPN	carbon paper		0.35		0.51		11.84
DMF	carbon paper	0.11	0.11	0.09	0.1	1.92	0.5
ACN	carbon paper	16.3	0.39	59.5	1.14	355.0	7.14
PC	carbon paper		0.43		1.0		1.3
DMSO	Cu complex-derived catalyst	0.31	0.15	0.32	0.09	0.94	0.18
MPN	Cu complex-derived catalyst		0.53		1.2		13.42
DMF	Cu complex-derived catalyst	5.43	0.23	28.85	0.52	296.4	5.83
ACN	Cu complex-derived catalyst	126.6	1.76	417.7	7.29	415.5	20.7
PC	Cu complex-derived catalyst	0.39	1.45	0.56	1.8	0.77	6.8

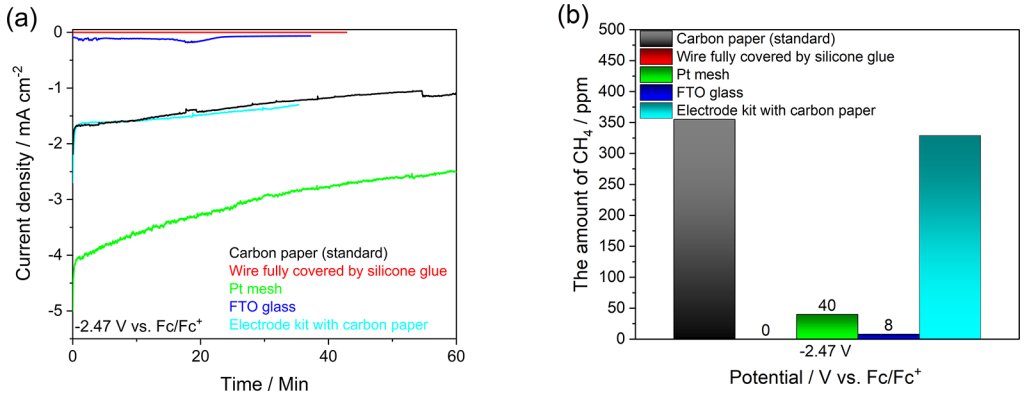

Figure 4. (a) Chronoamperogram at −2.47 V and (b) amount of methane produced on silicon glue, Pt mesh, FTO glass, and electrode kit with the carbon paper electrode in 0.1 M TBAP/ACN in argon.

respectively. In ACN, the amount of methane was much higher even only using the carbon paper electrode as compared to DMF and further increased significantly when the Cu complex-derived catalyst was used.

The origin of methane production using the carbon paper electrode can be assigned to solvent/electrolyte decomposition as previously suggested,[18] the decomposition of the carbon paper working electrode, or other components used to make the electrochemical cell. To check the possibility of methane production from other components, we have varied the fabrication of the electrochemical cell using the ACN-based electrolyte producing the largest amount of methane above. First, we tested whether the silicon glue used to isolate the copper tape from the electrolyte could release methane. We deposited the silicon glue directly onto the electric wire used for making the connections (see Figure S4). Second, a Pt mesh or an FTO glass was used as a working electrode instead of the carbon paper electrode to check whether the carbon paper working electrode is the possible carbon source of methane production. Third, we also changed the cell connections to check whether the use of copper tape/glue sealant played a role in methane generation, by directly attaching the carbon paper electrode to a Pt electrode using an electrode kit (see Figure S4). Only the carbon paper electrode was immersed in the electrolyte.

First, chronoamperometric experiments at −2.47 V using the wire covered by the silicone glue confirmed that it is not the source of the methane as there was close to zero current and no methane produced in argon (Figure 4a,b). Second, a high current density was obtained using a Pt mesh. Hydrogen was generated with nearly 90% FE with a partial current density (−2.34 mA cm^{-2}) but only 40 ppm of methane (partial current density, −0.24 mA cm^{-2}) was detected by the GC. The current density using the FTO glass working electrode, on the other hand, was very low (−0.063 mA cm^{-2}) at −2.47 V with 28 ppm of H_2 (30% FE) and 8 ppm of methane produced. The partial current density for the formation of CH_4 was −0.043 mA cm^{-2}. The amount of methane produced using the platinum electrode/FTO glass electrode and the partial current densities are well correlated with that of using the carbon paper electrode (*vide infra*); therefore, as expected for an inert electrode, carbon paper was not the source of methane. Third, CA using carbon paper connected by platinum using an electrode kit showed nearly identical current and the same amount of methane, confirming that the use of copper tape and silicon glue in our typical electrochemical setup did not contribute significantly to methane production.

The results of silicon glue and electrode kit with the carbon paper electrode confirm that methane was from solvent/electrolyte decomposition rather than the reactions with other components. Pt mesh and FTO glass produced methane during CA at −2.47 V in ACN even though the volume was very low compared to that of the carbon paper electrode. Pt mesh has large specific surface area, but it is known as a robust

https://doi.org/10.1021/acsomega.3c06440
ACS Omega 2023, 8, 41792−41801

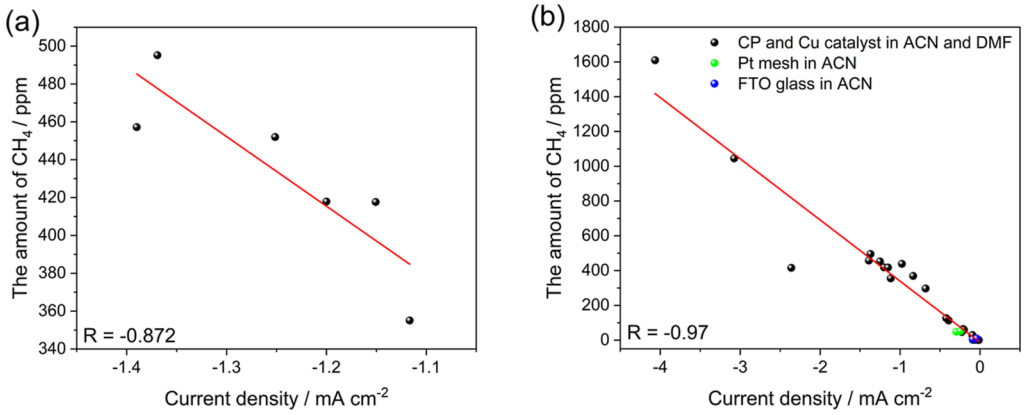

Figure 5. Linear correlation between current density and the amount of CH_4 produced (a) at −2.17 V using the Cu complex-derived catalyst and −2.47 V using the carbon paper electrode and (b) using all Cu complex-derived catalysts (Cu catalyst) and carbon paper electrodes (CP) in ACN and DMF and partial current densities and the amount of CH_4 at −2.47 V using Pt mesh and FTO glass in ACN.

catalyst for water reduction; therefore, H_2 was preferentially evolved rather than methane by solvent/electrolyte decomposition. Low volume of methane produced on FTO glass is due to the hydrophilic nature and smaller specific surface area. Thus, higher performance of solvent/electrolyte decomposition on the carbon paper electrode is due to large specific surface area and excellent wettability in organic solvents rather than methane generation by the carbon source of the carbon paper electrode.

Having confirmed that the source of methane production is not related to the decomposition of the carbon paper electrode or the components used to assemble the electrochemical cell, the remaining open question whether the increased methane production using the Cu complex-derived catalyst is solely related to accelerated electrolyte decomposition due to enhanced surface area (DMF) and/or catalytic activity (ACN) or the catalyst layer that likely contains some ligand-based organic phases may also contribute to methane production. To answer this question, we have correlated the amount of methane collected at various time stamps during CA with the current density measured at the sampling point for both the uncoated carbon paper electrode and the Cu complex-derived catalyst. First, the current density and the amount of CH_4 collected in the ACN-based electrolyte show a fairly strong correlation ($R = -0.872$) for data points measured using both Cu complex-derived catalysts and carbon paper electrodes (Figure 5a). This correlation suggests a similar mechanism of methane formation, i.e. the origin of the electrical current passed in the circuit is the same. Furthermore, linear correlation suggests that the same number of electrons is required to produce methane, and the slope does not change whether a catalyst layer is used or not. In other words, methane is generated by solvent/electrolyte decomposition. The role of the Cu complex-derived catalyst is lowering the overpotential for solvent/electrolyte decomposition in ACN or increasing the surface area (DMF) rather than the source of methane itself.

The high amount of methane produced in ACN-based electrolytes suggests that it is not a suitable electrolyte to evaluate the CO_2 reduction performance of the Cu complex-derived catalyst. Both carbon paper and Cu complex-derived catalysts produced some methane in DMF solvent at all potentials as well. The amount of charge during CA as well as the amount of methane was relatively small as compared to that of using ACN. Figure 5b shows a very strong correlation (R value of −0.97) between the current densities and the amount of methane produced in both DMF and ACN measured at three potentials. Two data points are added using the platinum and FTO working electrodes as shown in Figure 4 using the partial current densities at −2.47 V. The current densities and the amount of methane are listed in Table S1. The strong linear correlation independent of the solvent used implies that methane produced in DMF also originated from solvent/electrolyte decomposition. Although reaction mechanism is not clear, the same slope in the linear plot suggests that the same number of electrons is required by a solvent molecule to produce methane between ACN and DMF. In terms of practical applications, CO_2 reduction experiments using the Cu complex-derived catalyst in DMF-based electrolytes are probably acceptable at lower applied voltages as the amount of methane (∼28 ppm) at 2.17 V in an inert atmosphere was much smaller than that produced in a CO_2 atmosphere (506 ppm) at the same voltage. This background methane production may introduce ∼5% error in product selectivity. However, running the experiment over −2.47 V seems problematic due to the high volume of methane (355 ppm) produced by solvent/electrolyte decomposition in an inert atmosphere. These results strongly suggest that careful background measurement of using both the in situ-deposited catalyst and the uncoated electrodes is essential in organic solvents. The catalyst may enhance solvent/electrolyte decomposition by lowering the overpotential as in the case of ACN or can simply enhance the decomposition current due to the larger surface area (DMF).

In terms of DMSO, the very low current densities (∼0.03 mA cm^{-2}) and no gas products using both the Cu complex-derived catalyst and carbon paper electrode imply that no solvent/electrolyte decomposition occurred. On the other hand, high current densities (over −2 mA cm^{-2}) in MPN suggest electrolyte decomposition. However, the product could not be detected by GC and thus could be a liquid or a soluble organic product. In this case, product selectivity measurements in CO_2 reduction experiments would not be affected but the calculated FE would be lower.

To check whether the Cu complex-derived catalyst was transformed during chronoamperometric testing in argon, an ex situ analysis using CV measurements, XRD, and SEM was conducted. Figure S5 displays the CV curves of the Cu

https://doi.org/10.1021/acsomega.3c06440
ACS Omega 2023, 8, 41792−41801

complex-derived catalysts before and after CA in different solvent-based electrolytes. CV curves of the Cu complex-derived catalysts after CA in DMF, MPN, and DMSO showed increased capacitive current and similar redox peaks as compared to those before CA. The CV curve of the Cu complex-derived catalyst after CA in PC showed slightly decreased current density. The CV curve of the Cu complex-derived catalyst after CA in ACN showed an enhanced redox wave, showing the most significant changes as compared to before CA. Figure S6 shows similar XRD patterns of the Cu complex-derived catalysts before and after CA in different solvents. Additional peaks, not matched to patterns available in the XRD database, were detected after CA in DMF, ACN, and DMSO. Finally, notable morphological changes of the catalysts were observed in all solvents on the nano- to micrometer-scale before and after CA by using SEM (Figure S7). The original structure of the Cu complex-derived catalyst before CA showed small granular particles and rod-like shape in places. After CA, the Cu complex-derived catalyst after CA in DMF changed to a packed rod-like structure. Although the structure after CA in ACN appeared broadly similar to that of before CA, aggregation of small round particles (∼10 nm) was detected. The SEM image of the Cu complex-derived catalyst after CA in DMSO exhibited evenly distributed small granular particles (∼30 nm) as well as square-shaped particles (∼100 nm). The morphology of the sample after CA in MPN exhibited a very dense structure. The most significant structural change was found of the sample after CA in PC showing a 3D dendritic-like morphology.

The increased capacitive current of the carbon paper electrode after CA in all solvents suggests the enlargement of the electrochemically accessible surface area. Electrolyte access deeper into the pores of the carbon paper electrode, possibly by changing the wettability at highly reducing potentials, may be responsible for the increased accessible surface area. The increased capacitance of the electrodes coated with the Cu complex-derived catalyst in DMF, DMSO, and MPN could originate from the effect of adsorbed hydrogen (produced by water reduction).[32] Furthermore, it could also be related to catalyst restructuring as noted by SEM. The decrease in the capacitance of the Cu complex-derived catalyst after CA in PC could be correlated with the higher H_2 production rate of this system, i.e., more efficient release of H_2 and less H_2 adsorption on the surface. The enhancement of the redox wave of the Cu complex-derived catalyst after CA in ACN could suggest the change of the chemical composition of the catalyst during CA, i.e., deposition of some redox-active organic layer. Note that the XRD pattern of the metallic Cu phase remained similar.

During CA using the Cu complex-derived catalyst in DMF and ACN at −2.47 V, the amount of methane decreased over time (Figure S8), suggesting the deactivation of the catalyst as time progressed. SEM images showed the aggregation of some particles, which could be responsible for the reduced activity toward solvent/electrolyte decomposition together with the deposition of organic layers which may have lower catalytic activity or blocks the access of solvent to the catalytically active site.[26,27]

Testing the suitability of these solvent systems for CO_2 reduction experiments is beyond the current scope. We think the demonstrated experimental procedure is simple and requires only electrochemical/GC measurements already available in many CO_2 reduction setups. The correlation analysis is suggested to be a simple and straightforward way to prescreen organic solvents for CO_2 reduction experiments using in situ-deposited metal complex catalysts.

CONCLUSION

In summary, we have investigated whether the presence of an in situ-deposited catalyst in CO_2 reduction experiments using the Cu complex-based catalyst influences the catalytic decomposition of the solvent/electrolyte. We chose five well-known organic solvents known for their relatively wide potential window. In all five solvents, the current density was enhanced using a Cu complex-derived catalyst as compared to the uncoated carbon paper electrode. Importantly, a significant reduction of the onset potential was observed only in the ACN-based electrolyte, suggesting a catalytically enhanced solvent/electrolyte decomposition. In the other solvents including DMF, the enhanced current density is mostly attributed to the enhanced surface area, except for PC, in which the hydrogen evolution reaction with high FE was observed. A key finding of our work was a strong correlation between the measured current density and amount of methane produced independent of the solvent (DMF or ACN) or whether uncoated carbon electrodes or catalyst-coated electrodes were used, confirming that the source of methane is the solvent/electrolyte and not the catalyst layer itself. By checking other components of the electrochemical cell, we also confirmed that the working electrode or the method of cell assembly using a silicon glue-covered copper tape did not contribute to the methane production measurably. Using our Cu complex-derived catalysts, the use of ACN-based electrolyte should be avoided due to the high generation of methane under an inert argon atmosphere. DMF-based systems can be used if the voltage is limited to −2.17 V vs Fc/Fc^+ as the methane produced in an inert atmosphere is only 5% of the methane produced under CO_2 at this potential. In PC, both the Cu complex-derived catalyst and the carbon paper electrode produced hydrogen, while no gas products were detected in DMSO and MPN solvents, despite the latter having large current densities in chronoamperometric measurements. The study demonstrated a simple method to prescreen organic solvent-based electrolyte systems for reliable characterization of in situ-deposited metal complex-based catalysts for CO_2 reduction. Establishing the exact mechanism of solvent decomposition in the five solvent/electrolyte systems is beyond the scope of this work. Isotope labeling of the solvents and the electrolyte, systematically studying the effect of water content, ICP−MS analysis of the electrolyte, and monitoring of any liquid products should be all considered to establish the chemical mechanism in each electrolyte in future mechanistic studies.

ASSOCIATED CONTENT

Supporting Information

The Supporting Information is available free of charge at https://pubs.acs.org/doi/10.1021/acsomega.3c06440.

Electrodeposition curves, electrochemical measurement procedures and preparation of the working electrode, five cycles of CV of Cu complex-derived catalysts in five different solvents, list of the amount of methane and current densities measured using carbon electrodes and Cu complex-derived catalysts, CV curves before and after CA using Cu complex-derived catalysts, XRD patterns of Cu complex-derived catalysts before and after

https://doi.org/10.1021/acsomega.3c06440
ACS Omega 2023, 8, 41792−41801

CA, and SEM images of Cu complex-derived catalysts before and after CA (PDF)

AUTHOR INFORMATION

Corresponding Author

Attila J. Mozer − *Intelligent Polymer Research Institute and ARC Centre of Excellence for Electromaterials Science, University of Wollongong, Wollongong, New South Wales 2522, Australia;* orcid.org/0000-0002-8500-606X; Email: attila@uow.edu.au

Authors

Kyuman Kim − *Intelligent Polymer Research Institute and ARC Centre of Excellence for Electromaterials Science, University of Wollongong, Wollongong, New South Wales 2522, Australia;* orcid.org/0000-0002-6506-7623

Pawel Wagner − *Intelligent Polymer Research Institute and ARC Centre of Excellence for Electromaterials Science, University of Wollongong, Wollongong, New South Wales 2522, Australia;* orcid.org/0000-0003-1926-9862

Klaudia Wagner − *Intelligent Polymer Research Institute and ARC Centre of Excellence for Electromaterials Science, University of Wollongong, Wollongong, New South Wales 2522, Australia;* orcid.org/0000-0001-6803-4221

Complete contact information is available at: https://pubs.acs.org/10.1021/acsomega.3c06440

Notes

The authors declare no competing financial interest.

ACKNOWLEDGMENTS

Funding from the Australian Research Council Centre of Excellence Scheme (Project Number CE 140100012) is gratefully acknowledged. The authors would like to thank the Australian National Fabrication Facility−Materials node for equipment use.

REFERENCES

(1) Azcarate, I.; Costentin, C.; Robert, M.; Savéant, J. M. Dissection of electronic substituent effects in multielectron−multistep molecular catalysis. Electrochemical CO_2-to-CO conversion catalyzed by iron porphyrins. *J. Phys. Chem. C* **2016**, *120* (51), 28951−28960.

(2) Smieja, J. M.; Kubiak, C. P. Re (bipy-tBu)$(CO)_3$Cl− improved catalytic activity for reduction of carbon dioxide: IR-spectroelectrochemical and mechanistic studies. *Inorg. Chem.* **2010**, *49* (20), 9283−9289.

(3) Kim, K.; Wagner, P.; Wagner, K.; Mozer, A. J. Electrochemical CO_2 Reduction Catalyzed by Copper Molecular Complexes: The Influence of Ligand Structure. *Energy Fuels* **2022**, *36* (9), 4653−4676.

(4) Zhu, Q.; Sun, X.; Yang, D.; Ma, J.; Kang, X.; Zheng, L.; Zhang, J.; Wu, Z.; Han, B. Carbon dioxide electroreduction to C_2 products over copper-cuprous oxide derived from electrosynthesized copper complex. *Nat. Commun.* **2019**, *10* (1), 3851.

(5) Rooney, C. L.; Wu, Y.; Gallagher, D. J.; Wang, H. Restructuring and integrity of molecular catalysts in electrochemical CO_2 reduction. *Nat. Sci.* **2022**, *2* (4), No. e20210628.

(6) Kortlever, R.; Shen, J.; Schouten, K. J. P.; Calle-Vallejo, F.; Koper, M. T. Catalysts and reaction pathways for the electrochemical reduction of carbon dioxide. *J. Phys. Chem. Lett.* **2015**, *6* (20), 4073−4082.

(7) Xu, Y.; Li, F.; Xu, A.; Edwards, J. P.; Hung, S.-F.; Gabardo, C. M.; O'Brien, C. P.; Liu, S.; Wang, X.; Li, Y.; et al. Low coordination number copper catalysts for electrochemical CO_2 methanation in a membrane electrode assembly. *Nat. Commun.* **2021**, *12* (1), 2932.

(8) Peterson, A. A.; Nørskov, J. K. Activity descriptors for CO_2 electroreduction to methane on transition-metal catalysts. *J. Phys. Chem. Lett.* **2012**, *3* (2), 251−258.

(9) Weng, Z.; Wu, Y.; Wang, M.; Jiang, J.; Yang, K.; Huo, S.; Wang, X.-F.; Ma, Q.; Brudvig, G. W.; Batista, V. S.; et al. Active sites of copper-complex catalytic materials for electrochemical carbon dioxide reduction. *Nat. Commun.* **2018**, *9* (1), 415.

(10) Zhang, H.; Yang, Y.; Liang, Y.; Li, J.; Zhang, A.; Zheng, H.; Geng, Z.; Li, F.; Zeng, J. Molecular Stabilization of Sub-Nanometer Cu Clusters for Selective CO_2 Electromethanation. *ChemSusChem* **2022**, *15* (1), No. e202102010.

(11) Simpson, T. C.; Durand, R. R. Ligand participation in the reduction of CO_2 catalyzed by complexes of 1, 10 o-phenanthroline. *Electrochim. Acta* **1988**, *33* (4), 581−583.

(12) König, M.; Vaes, J.; Klemm, E.; Pant, D. Solvents and supporting electrolytes in the electrocatalytic reduction of CO_2. *Iscience* **2019**, *19*, 135−160.

(13) Sargeant, E.; Rodríguez, P. Electrochemical conversion of CO_2 in non-conventional electrolytes: Recent achievements and future challenges. *Electrochem. Sci. Adv.* **2022**, *3*, No. e2100178.

(14) Gong, K.; Fang, Q.; Gu, S.; Li, S. F. Y.; Yan, Y. Nonaqueous redox-flow batteries: organic solvents, supporting electrolytes, and redox pairs. *Energy Environ. Sci.* **2015**, *8* (12), 3515−3530.

(15) Zhang, D.; Chen, J.; Hao, Z.; Jiao, L.; Ge, Q.; Fu, W.-F.; Lv, X.-J. Highly efficient electrochemical hydrogenation of acetonitrile to ethylamine for primary amine synthesis and promising hydrogen storage. *Chem Catal.* **2021**, *1* (2), 393−406.

(16) Pons, S.; Khoo, S. Reductions in aprotic media-I. Cathodic reduction limits at a platinum electrode in acetonitrile. *Electrochim. Acta* **1982**, *27* (9), 1161−1169.

(17) Foley, J. K.; Korzeniewski, C.; Pons, S. Anodic and cathodic reactions in acetonitrile/tetra-n-butylammonium tetrafluoroborate: an electrochemical and infrared spectroelectrochemical study. *Can. J. Chem.* **1988**, *66* (1), 201−206.

(18) Hoshi, N.; Harada, T.; Nakamura, M.; Nozu, D. Enhancement of toluene formation by water during electrolysis of chlorobenzene at Pt electrode in acetonitrile. *Electrochemistry* **2007**, *75* (9), 715−718.

(19) Szklarczyk, M.; Sobkowski, J. The behaviour of high polar organic solvents at platinum electrode—II. Adsorption and electrode reactions of acetonitrile. *Electrochim. Acta* **1980**, *25* (12), 1597−1601.

(20) Ue, M.; Ida, K.; Mori, S. Electrochemical properties of organic liquid electrolytes based on quaternary onium salts for electrical double-layer capacitors. *J. Electrochem. Soc.* **1994**, *141* (11), 2989−2996.

(21) Kim, K.; Wagner, P.; Wagner, K.; Mozer, A. J. Electrochemical CO_2 Reduction to Methane by Cu complex-derived Catalysts in Non-aqueous Media. *ChemCatChem* **2023**, *15*, No. e202300396.

(22) Luca, O. R.; Gustafson, J. L.; Maddox, S. M.; Fenwick, A. Q.; Smith, D. C. Catalysis by electrons and holes: formal potential scales and preparative organic electrochemistry. *Org. Chem. Front.* **2015**, *2* (7), 823−848.

(23) Popović, S.; Smiljanić, M.; Jovanovič, P.; Vavra, J.; Buonsanti, R.; Hodnik, N. Stability and degradation mechanisms of copper-based catalysts for electrochemical CO_2 reduction. *Angew. Chem.* **2020**, *132* (35), 14844−14854.

(24) Hori, Y.; Konishi, H.; Futamura, T.; Murata, A.; Koga, O.; Sakurai, H.; Oguma, K. Deactivation of copper electrode" in electrochemical reduction of CO_2. *Electrochim. Acta* **2005**, *50* (27), 5354−5369.

(25) Kim, D.; Kley, C. S.; Li, Y.; Yang, P. Copper nanoparticle ensembles for selective electroreduction of CO_2 to C_2−C_3 products. *Proc. Natl. Acad. Sci. U.S.A.* **2017**, *114* (40), 10560−10565.

(26) Reller, C.; Krause, R.; Volkova, E.; Schmid, B.; Neubauer, S.; Rucki, A.; Schuster, M.; Schmid, G. Selective electroreduction of CO_2 toward ethylene on nano dendritic copper catalysts at high current density. *Adv. Energy Mater.* **2017**, *7* (12), 1602114.

(27) Jung, H.; Lee, S. Y.; Lee, C. W.; Cho, M. K.; Won, D. H.; Kim, C.; Oh, H.-S.; Min, B. K.; Hwang, Y. J. Electrochemical fragmentation

of Cu_2O nanoparticles enhancing selective C−C coupling from CO_2 reduction reaction. *J. Am. Chem. Soc.* **2019**, *141* (11), 4624−4633.
(28) Hashmi, S. G.; Sonai, G. G.; Iftikhar, H.; Lund, P. D.; Nogueira, A. F. Printed single-walled carbon-nanotubes-based counter electrodes for dye-sensitized solar cells with copper-based redox mediators. *Semicond. Sci. Technol.* **2019**, *34* (10), 105001.
(29) Du, J.; Cheng, B.; Jiang, L.; Han, Z. Copper phenanthroline for selective electrochemical CO_2 reduction on carbon paper. *Chem. Commun.* **2023**, *59* (32), 4778−4781.
(30) Xie, Y.; Du, H. Electrochemical capacitance of a carbon quantum dots-polypyrrole/titania nanotube hybrid. *RSC Adv.* **2015**, *5* (109), 89689−89697.
(31) Zhang, L.; Xiao, J.; Wang, H.; Shao, M. Carbon-based electrocatalysts for hydrogen and oxygen evolution reactions. *ACS Catal.* **2017**, *7* (11), 7855−7865.
(32) Kaur, M.; Pal, K. Review on hydrogen storage materials and methods from an electrochemical viewpoint. *J. Energy Storage* **2019**, *23*, 234−249.

https://doi.org/10.1021/acsomega.3c06440
ACS Omega 2023, 8, 41792−41801